Available online at www.sciencedirect.com

ScienceDirect

Developmental Biology 309 (2007) 180–192

DEVELOPMENTAL BIOLOGY

www.elsevier.com/developmentalbiology

The zebrafish *runzel* muscular dystrophy is linked to the titin gene

Leta S. Steffen [a,*], Jeffrey R. Guyon [a], Emily D. Vogel [a], Melanie H. Howell [a], Yi Zhou [b,c,d], Gerhard J. Weber [b,c,d], Leonard I. Zon [b,c,d,e], Louis M. Kunkel [a,e]

[a] *Department of Genetics, Harvard Medical School, and Program in Genomics, Children's Hospital, 300 Longwood Ave., Boston, MA, USA*
[b] *Stem Cell Program, Children's Hospital, Boston, MA, USA*
[c] *Harvard Stem Cell Institute, Harvard Medical School, Boston, MA, USA*
[d] *Division of Hematology/Oncology, Children's Hospital and Dana Farber Cancer Institute, Boston, MA, USA*
[e] *Howard Hughes Medical Institute, Harvard Medical School, Boston, MA, USA*

Received for publication 9 January 2007; revised 15 May 2007; accepted 20 June 2007
Available online 23 June 2007

Abstract

Titin (also called connectin) acts as a scaffold for signaling proteins in muscle and is responsible for establishing and maintaining the structure and elasticity of sarcomeres in striated muscle. Several human muscular dystrophies and cardiomyopathies have previously been linked to mutations in the titin gene. This study reports linkage of the *runzel* homozygous lethal muscular dystrophy in the zebrafish *Danio rerio* to a genomic interval containing the titin gene. Analysis of the genomic sequence suggests that zebrafish contain two adjacent titin loci. One titin locus lies within the genetic linkage interval and its expression is significantly reduced in *runzel* mutants by both immunofluorescence and protein electrophoresis. Morpholino downregulation of this same titin locus in wild-type embryos results in decreased muscle organization and mobility, phenocopying *runzel* mutants. Additional protein analysis demonstrates that, in wild-type zebrafish, titin isoform sizes are rapidly altered during the development of striated muscle, likely requiring a previously unrecognized need for vertebrate sarcomere remodeling to incorporate developmentally regulated titin isoforms. Decreases of affected titin isoforms in *runzel* mutants during this time correlate with a progressive loss of sarcomeric organization and suggest that the unaffected titin proteins are capable of sarcomerogenesis but not sarcomere maintenance. In addition, microarray analysis of the *ruz* transcriptome suggests a novel mechanism of dystrophy pathogenesis, involving mild increases in calpain-3 expression and upregulation of heat shock proteins. These studies should lead to a better understanding of titin's role in normal and diseased muscle.

Keywords: Titin; Muscular dystrophy; Titinopathy; Birefringence; Zebrafish; Zebrafish muscle; Sarcomere

Introduction

Titin is the largest known protein with major isoforms estimated at 3–4 MDa (Bang et al., 2001). Originally named connectin, titin was identified by Maruyama (1976) as a major filamentous protein of the sarcomere present in all striated muscle. The sarcomere is the repeated structural unit of contraction and relaxation in striated muscle and appears in electron micrographs as an alternating series of parallel Z and M line structures. Actin-thin filaments and myosin-thick filaments extend perpendicularly from the Z and M lines, respectively. During muscle contraction, myosin-thick filaments slide toward the Z line along thin filaments, shortening sarcomere length. Single titin proteins have been measured at greater than 1 μm and stretch the entire distance of the half-sarcomere, with amino termini localized to the Z line and carboxy termini at the M line (Furst et al., 1988).

Titin is vital to muscle architecture and signaling in both developing and mature striated muscle. In vitro experiments using cell lines with partial titin deletions suggest that titin is required for skeletal muscle sarcomerogenesis, providing a scaffold for organization and spacing of nascent Z line and M line structures (Miller et al., 2003; van der Ven et al., 2000). In mature muscle, titin plays a similar role, maintaining M line width and localization (Gregorio et al., 1998; Obermann et al., 1996). Titin has also been shown to provide much of the passive tension and elasticity of muscle fibers through the unfolding of a

* Corresponding author.
E-mail address: lsteffen@gmail.com (L.S. Steffen).

0012-1606/$ - see front matter © 2007 Elsevier Inc. All rights reserved.
doi:10.1016/j.ydbio.2007.06.015

unique I-band region (called the PEVK) (Freiburg et al., 2000). In addition to these structural roles, titin contains a myosin-light chain-like kinase domain as well as binding sites for calcium and more than 15 known proteins, many of which play roles in muscle signaling events (Tskhovrebova and Trinick, 2004). Mutations in several of these binding partners, including the muscle-specific protease calpain-3, have also been linked to muscular dystrophies, suggesting a central role for titin-associated signaling pathways in muscle physiology.

The titin gene (*TTN*) contains over 360 exons that give rise to multiple splice isoforms, varying in size with the organism, muscle, stage of development, and disease state (Bang et al., 2001; Nagueh et al., 2004; Warren et al., 2003a, 2004). Much of this variation has been attributed to differential splicing of the approximately 300 total immunoglobulin and fibronectin repeats, though the function of such variation is unknown. Splicing to include variable numbers of titin Z-repeats has been detected and may regulate Z line morphology (Gregorio et al., 1998). Additional splice variants in the PEVK exons correlate with alteration of myofibrillar passive tension and stiffness of myofibers in both cardiac and skeletal muscle (Cazorla et al., 2000; Lahmers et al., 2004; Prado et al., 2005). And cardiac isoforms differ from skeletal muscle titin by the inclusion of the N2B exon, a cardiac-specific titin exon.

Titin's importance in muscle regulation has been highlighted by the five human diseases now linked to titin mutations. While none of the mutations affecting skeletal muscle appear to modify titin localization, overall muscle function is severely affected, likely through alteration of titin-associated signaling pathways. Two diseases of the skeletal muscle – tibial muscular dystrophy (TMD) and limb girdle muscular dystrophy 2J (LGMD2J) – result from mutations in the M line region of titin that prevent binding of the protease, calpain-3 (Hackman et al., 2002; Haravuori et al., 2001). A murine titin mutation disrupts binding of calpain-3 to a second site, resulting in the severe muscular dystrophy with myositis (*mdm*) phenotype (Huebsch et al., 2005; Witt et al., 2004). All three titin mutations decrease or eliminate calpain-3 expression in muscle, though studies in the *mdm* mouse suggest that this is not the only signaling pathway affected. The third skeletal muscle disease, hereditary myopathy with early respiratory failure (HMERF), results from a mutation in the titin kinase domain that affects alternative titin-associated signaling pathways, leading to downregulation of muscle gene transcription (Lange et al., 2005). Familial dilated cardiomyopathy (DCM) has also been linked to several different titin mutations (Gerull et al., 2006; Itoh-Satoh et al., 2002; Knoll et al., 2002).

The zebrafish *Danio rerio* has recently emerged as a promising organism for the study of vertebrate muscle development and disease. During early embryonic stages, zebrafish are composed largely of skeletal muscle that can contract by 24 hours post-fertilization (hpf) and is responsive shortly after 36 hpf (Kimmel et al., 1995). Expression of human muscle homologs, including sarcomeric and sarcolemmal proteins, has been confirmed by genome analysis and immunofluorescent studies (Bassett and Currie, 2003; Costa et al., 2002). In addition, two human muscular dystrophies have been at least partially replicated in zebrafish by downregulating zebrafish homologs of dystrophy-associated genes, suggesting conservation of their functional roles within muscle (Dodd et al., 2004; Guyon et al., 2003, 2005). Finally, the zebrafish mutant pickwick (pik^{m171}) has been mapped to the cardiac-specific N2B exon of titin. pik^{m171} mutants have been suggested as a model for DCM and show a primary failure in cardiac sarcomerogenesis, suggesting that zebrafish titin orthologs play analogous roles to mammalian titin during sarcomere development (Xu et al., 2002). The cardiac specificity of pik^{m171} suggests that zebrafish titin may also yield multiple splice isoforms.

In 1996, a chemical mutagenesis screen by the Tuebingen laboratories generated four mutants with muscular dystrophy phenotypes. One of these has been mapped to dystrophin, mutations in which cause Duchenne and Becker muscular dystrophies in humans (Bassett et al., 2003; Granato et al., 1996). *runzel* (*ruz*), a second Tuebingen dystrophic mutant, was characterized with grossly normal muscle structure and function at 2 dpf but poor swimming ability and decreased birefringence at 5 dpf, indicating progressive loss of muscle organization. We have now genetically mapped the *ruz* mutation to a region on chromosome (Chr) 9 containing the titin gene. Further work suggests that the zebrafish titin locus is duplicated with only one copy located within the genetically linked region. Muscle function and organization defects seen in *ruz* mutants can be phenocopied by antisense morpholinos directed against the linked titin locus. India ink stain of electrophoretically separated proteins demonstrates that the titin isoforms expressed by wild-type skeletal muscle change at several points during early embryonic development, with at least 9 distinct sizes detected. In *ruz* mutants, expression of certain isoforms is reduced. While the remaining titin isoforms are sufficient for sarcomerogenesis, electron microscopy shows that they are not sufficient for maintenance of myofibrillar organization in the *ruz* mutants. In addition, decreases in known titin-associated pathways were not detected in the *ruz* mutant. Instead, microarray analysis suggests increases in transcripts of several muscle genes and heat shock proteins. This work suggests that alterations in titin can lead to a novel skeletal muscular dystrophy-like phenotype. In addition, it demonstrates a previously unrecognized rapid turnover in titin isoforms during skeletal muscle development and suggests separable functions of these titin isoforms.

Materials and methods

Fish maintenance and mutant identification

The *ruz* mutation tk258a was isolated as part of an ENU mutagenesis screen (Granato et al., 1996) and is maintained on the TL background. To generate families for linkage analysis, *ruz* heterozygotes were mated pairwise with wild-type WIK fish. F1 mapping heterozygotes were identified from these families and mated pairwise. Homozygous mutant F2 offspring were identified based on decreased birefringence at 3–10 dpf as previously described (Granato et al., 1996). All animal work was performed with approval from the Children's Hospital Animal Care and Use Committee (Protocol #A03-11-080).

Immunofluorescence and hematoxylin staining

Five to 7 dpf *ruz* mutants and wild-type siblings or 3.5 dpf TTN_1 morphants and control siblings were fixed in 4% paraformaldehyde, infiltrated with 20%

sucrose in PBS, embedded in OCT (TissueTek), and frozen in nitrogen-cooled 2-methylbutane. Samples were longitudinally sectioned to 8 μm. Hematoxylin staining was performed and coverslips mounted with Vectashield (Vector Labs). On additional sections, immunofluorescence was performed using the following antibodies singly or in pairs: anti-titin T11 (Sigma), actin A2066 (Sigma), nebulin N2B (Sigma), β-dystroglycan (Novocastra), MuRF2 (GeneTex), and MuRF1 (GeneTex). Samples were washed and incubated with appropriate secondary antibodies (Jackson Immunolabs). Coverslips were mounted using Vectashield with DAPI (Vector Labs) and slides were viewed at 100× or 400× using a Nikon Eclipse E1000 fluorescent microscope. Images were collected with a Hamamatsu ORCA-ER camera and OpenLab3.1.5 software at the same length exposure time for each antibody set. Hematoxylin-stained samples were viewed at 400× and images collected with a SPOT InSight QE camera (Diagnostics Instruments, Inc.).

Electrophoresis, India ink, and Western blot analysis

Equal weights of whole 2 dpf, 3.5 dpf, or 6.5 dpf fish were Dounce homogenized in lysis buffer (500 mM Tris pH 7.4, 150 mM NaCl, 1% NP-40, 1 mM PMSF, 0.1% SDS, 1× protease inhibitor cocktail; Roche) on ice and centrifuged at 14,000×*g* for 10 min at 4 °C. Autopsy tissue from human psoas muscle was similarly prepared. Prior to electrophoresis, denaturing buffer (8 M urea, 2 M thiourea, 3% SDS, 75 mM DTT, 0.1% bromophenol blue, 0.05% Tris–Cl pH 6.8) was added 4:1 to lysates. Samples were denatured at 60 °C for 10 min and vortexed. Electrophoresis using a denaturing 1% agarose gel was performed as previously described (Warren et al., 2003b). Equal volumes of protein lysates or equal total protein amounts from each sample were separated by electrophoresis at 15 mA for 4.5 h and transferred to nitrocellulose membranes in transfer buffer (25 mM Tris base, 192 mM glycine, 10% methanol) for 3 h at maximum voltage (16–22 V). Membranes were washed in PBS + 0.3% Tween, incubated overnight in 0.1% India ink, and then rinsed with water. Lysates for Western blot analysis of all smaller proteins were prepared, separated by electrophoresis on 3–8% Tris–acetate gels (Invitrogen), transferred to nitrocellulose, and immunoblotted as previously described with NCL-CALP-12A2 (Novocastra) or actin A2066 (Sigma) antibodies (Guyon et al., 2005).

Genetic mapping

Genetic mapping families were generated as indicated above and F2 wild-type and *ruz* mutants collected. DNA preparation and bulk segregant analysis was performed as previously described (Bahary et al., 2004; Shepard et al., 2005) using agarose-scorable length polymorphisms of 239 microsatellites on pools of wild-type or mutant DNA. Polymorphisms were detected by electrophoresis of PCR products for 2–2.5 h at 230V on a gel of 1% GenePureLE Agarose and 1% Hi-Res GenePure Agarose mix. Further linkage analysis was performed on DNA of individual embryos using primers designed to additional Chr 9 microsatellites identified from the Massachusetts General Hospital Zebrafish Server (http://zebrafish.mgh.harvard.edu).

To create a contig for higher resolution mapping, protein sequences of non-repetitive human cardiac titin exons (NM_003319) were mapped *in silico* to finished clones in the Sanger Center database (www.sanger.ac.uk as of 2003/27/05) using the tblastn algorithm. Resulting BACs were aligned using Sequencher (Gene Codes). The BAC contig was extended to z14949 *in silico* using BAC end sequence. Microsatellites for higher resolution mapping were identified using SSR identification software at danio.mgh.harvard.edu/markers/ssr.html. The following primer sequences were used:

RuzB (forward): 5′-CCTCACCAGGGATACCCTTA-3′
RuzB (reverse): 5′-TGGTGATCAGGTGTGCAGTT-3′
RuzD (forward): 5′-GGGGATGTTAGGCAGTCAGA-3′
RuzD (reverse): 5′-TTCCAAACACCCATAGGTCA-3′
RuzH (forward): 5′-CTTGTGCAGAAATCGCCAAT-3′
RuzH (reverse): 5′-AGGAGGCCTCTGATGTAGGA-3′.

Morpholino injections

The translation start site for the TTN_1 gene was identified by orthology to human titin protein (tblastn with exon 2 of NM_13378) and two non-overlapping translation start site morpholinos were designed (GeneTools). The sequence of morpholino TTN1a was 5′-TAAATGTTGGAGCTTGCGTTGACAT-3′ and the accompanying inverted control was 5′-TACAGTTGCGTTCGAGGTTGTA-AAT-3′. Morpholino TTN1b was 5′-TGTATCACAAGGTTGCCTACACTTG-3′. Zebrafish embryos were injected at the 1- to 4-cell stage with approximately 10 ng of antisense morpholino or the inverted control morpholino and raised at 28.5 °C until analysis as above. Isogenic uninjected embryos from the same clutches were also analyzed as a control.

Electron microscopy

Skeletal muscle of *ruz* mutant and wild-type siblings at 3.5 or 6.5 dpf was fixed overnight at 4 °C in 100 mM cacodylate buffer with 1.25% formaldehyde, 2.5% glutaraldehyde, and 0.03% picric acid. Samples were then processed by the Harvard Medical School EM Facility as follows: Muscles were post-fixed in 1% osmiumtetroxide/1.5% potassiumferrocyanide, stained with 1% uranyl acetate in maleate buffer (pH 5.2), and dehydrated in graded ethanols. Following dehydration, samples were incubated in propyleneoxide and infiltrated with a 1:1 mixture of Epon (Marivac Ltd.) and propyleneoxide overnight before embedding in fresh Epon. Longitudinal muscle sections (80–90 nm) were mounted on formvar/carbon-coated copper grids, stained with 2% uranyl acetate in acetone, and then in 0.2% lead citrate. Sections were viewed with a JEOL 1200EX transmission electron microscope at 80 kV.

RNA expression analysis

For all mRNA analysis, 3.5 dpf *ruz* mutants and wild-type siblings were quickly dissected to remove head, heart, and gut from skeletal muscle of the trunk and tail. Pooled muscle was homogenized by douncing in Buffer RLT (Qiagen) and centrifuging through a QiaShredder column (Qiagen). RNA was extracted from homogenates using either the Qiagen RNeasy or RNeasy Micro kit with an on-column DNase step. For microarray analysis, mutant RNA was matched with RNA of wild-type siblings from the same clutch. Three separate clutches were used ($n=3$). cRNA was produced and hybridized to Affymetrix zebrafish Gene Chips as previously described (Shepard et al., 2005). Data were analyzed using Affymetrix Microarray Suite software with additional custom software according to Choe et al. (2005) and Weber et al. (2005). Resulting probes with $q \leq 0.05$ and a fold change =1.6 were annotated using the blastn algorithm to compare probe consensus sequences with zebrafish ESTs and tblastx between the probe consensus/EST sequences and human sequences.

Quantitative RT-PCR was used to confirm a decrease in transcripts containing the Dr.1662 probe consensus sequence and to analyze changes in zebrafish CARP and ankrd2 levels. cDNA was synthesized from 1 μg of RNA in a 25-μL reaction volume using a Superscript II kit (Invitrogen) with an oligo(dT) primer according to the manufacturer's instructions. Quantitative PCR was performed with 1 μL of cDNA using SYBR Green PCR Master Mix (Applied Biosystems) and an ABI Prism 7700 Sequence Detector. Transcript expression was normalized to internal control expression levels (Tbp).

Results

Phenotypic characterization of ruz

runzel (*ruz*) is a recessive zebrafish dystrophy mutation identified as part of a Tuebingen ENU mutagenesis screen (Granato et al., 1996). The *ruz* phenotype is first apparent at 3–3.5 dpf as decreased birefringence of somitic muscle indicating decreased muscle organization (Fig. 1). Birefringence is used to assess muscle organization based on the ability of highly ordered sarcomeres to rotate polarized light. By 5 dpf, mutants also lack an inflated swim bladder, show decreased motility, and are unable to swim normally. Mutants on a Tuebingen background frequently demonstrated a curvature of the body

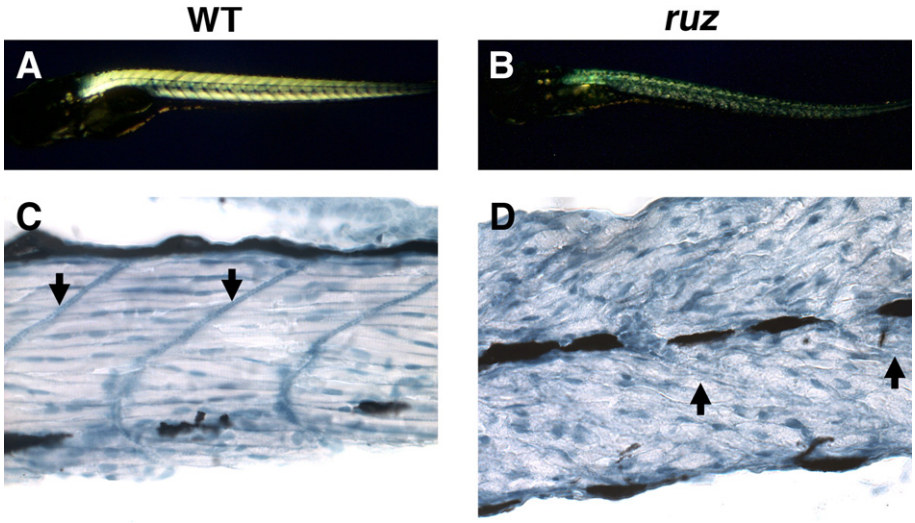

Fig. 1. Skeletal muscle is severely disorganized in *ruz* mutants. (A) Wild-type fish skeletal muscle is highly birefringent at 5–6 dpf. (B) 5–6 dpf *ruz* homozygous mutants show decreased skeletal muscle birefringence and, on a TL background, body curvature. (C, D) Longitudinal sections of zebrafish skeletal muscle at 5 dpf were stained with hematoxylin. (C) Wild-type muscle shows myofiber alignment between myosepta and peripherally localized nuclei. (D) *ruz* muscle myofibers appear unaligned with abnormally shaped nuclei. Arrows indicate myosepta.

and poor body posture while resting (Fig. 1B). By 6–7 dpf, *ruz* mutants are only able to produce a shuddering motion of the tail and continue to display decreased birefringence (Figs. 1A, B). No cardiac abnormalities were detected, suggesting a skeletal muscle-specific phenotype. Homozygosity of the mutation is lethal at 10–12 dpf, while heterozygotes show no gross abnormalities in swimming ability, mating, or lifespan (data not shown).

Examination of hematoxylin-stained *ruz* mutants confirms that skeletal muscle myofibers are severely disorganized. In wild-type fish embryos, myofibers are aligned roughly parallel to the body axis of the fish, stretching between adjacent myosepta (Fig. 1C). At 5 dpf, most myofibers are multinucleate with nuclei flattened and aligned along the fiber periphery, similar to mammalian myofiber organization. *ruz* mutants, however, show no apparent alignment of the myofibers at 6–7 dpf, and nuclei are frequently abnormally shaped (Fig. 1D).

To determine functional changes in *ruz* skeletal muscle, several muscle proteins were examined for differences in expression. Nearly all sarcolemmal proteins analyzed by immunofluorescence localized to the myosepta in wild-type embryonic zebrafish muscle and were unaffected in *ruz* mutants (Figs. 2A–D, and data not shown). It thus appears that myosepta are maintained, though they appear disorganized by hematoxylin assessment (Fig. 1D). Immunofluorescence using antibodies against sarcomeric proteins, however, suggests disruption of the basic contractile apparatus in *ruz* mutants. Nebulin is a major filamentous protein of striated muscle and is found on either side of the Z line in wild-type embryos (Fig. 2E). In *ruz* mutants, sarcomeric staining of nebulin is severely decreased at 5–7 dpf (Fig. 2F), though overall expression appears consistent by immunoblot analysis (data not shown). Similarly, expression of sarcomeric actin (Figs. 2G, H) is maintained in *ruz* mutants but few striations are apparent, suggesting a primary failure at the sarcomere.

ruz mutants have a defect in titin

Genetic linkage analysis was initially performed by comparing inheritance of polymorphic microsatellite markers between pools of wild-type and *ruz* mutant DNA. This bulk segregant analysis suggested linkage to chromosome (Chr) 9. The mutation was further mapped by linkage analysis on individual genomes to an interval between genetic markers z14949 and z26463 (Fig. 3A). This region of Chr 9 is syntenic with Chr 2 in humans and contains the giant muscle gene, titin (*TTN*) (Sato and Mishina, 2003; Xu et al., 2002). However, the zebrafish genome in this region of Chr 9 showed a high degree of misassembly at that time.

Previous studies have shown zebrafish cardiac titin to be highly homologous to human cardiac titin (Xu et al., 2002). In order to establish sequence within the linked genomic interval, human cardiac titin exons with non-repetitive sequences were used to identify zebrafish BACs from the Sanger Center zebrafish database. Seven BACs were identified and aligned to create a contig across the titin locus (Fig. 3B). Again using the Sanger Center database, this contig was extended *in silico* to one of the flanking microsatellites (Fig. 3B). Careful alignment of the human titin N2B cardiac or N2A skeletal muscle isoform sequences with the zebrafish BAC contig suggests genomic duplication of the titin locus in zebrafish (designated TTN_1 and TTN_2) that is also supported by the most recent zebrafish genomic alignment (Fig. 3C and Zv6 of the Sanger Centre Zebrafish Genome). The adjacent titin gene loci are divergent at both the nucleotide and protein levels, suggesting that the duplication is not just due to a misalignment of BAC sequences. Duplication is further supported by linkage analysis using microsatellites located within and flanking the duplicated genes (data not shown). Microarray analysis performed on wild-type and *ruz* embryos suggests that transcripts can be expressed from both loci (Fig. 3, Table 1).

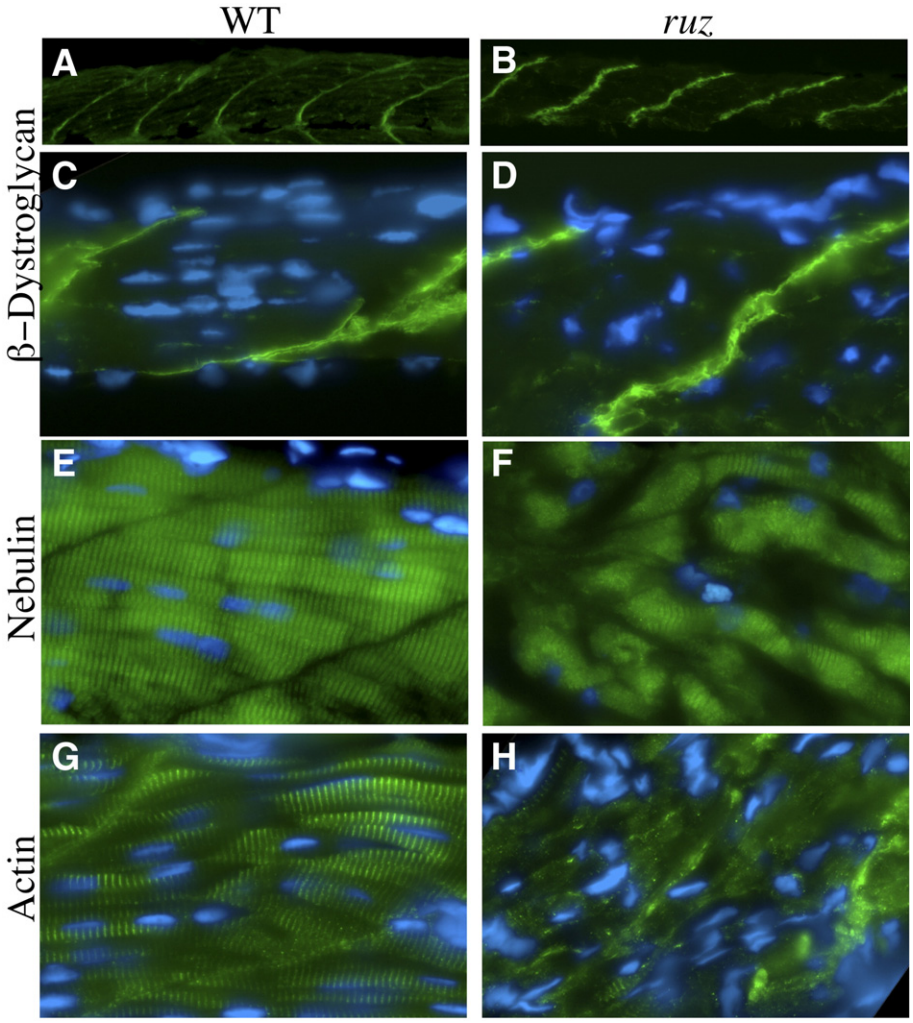

Fig. 2. Sarcomeric proteins are mislocalized in *ruz* mutant skeletal muscle. Indirect immunofluorescence was performed on longitudinal sections of 5–6 dpf mutant and wild-type skeletal muscle and samples were imaged at 100× (A, B) or 400× (C–F). (A, C) β-Dystroglycan protein localizes to the myosepta of wild-type embryonic muscle. (B, D) In *ruz* mutants, β-dystroglycan is maintained at the myosepta. (C) Nebulin localizes to the sarcomere in wild-type embryos. (D) Nebulin sarcomeric localization is lost throughout most of *ruz* mutant muscle. (E) Skeletal muscle actin similarly localizes to the sarcomere in wild-type embryos while localization is lost in *ruz* mutants (F). Nuclei were stained with DAPI (blue).

Additional microsatellites for high resolution mapping were identified throughout the BAC contig and *ruz* mutants and wild-type siblings were tested for agarose-scorable linkage. Recombination events in 4 out of 1486 meioses further narrowed the region of linkage to less than 0.3 cm between microsatellites B and H, representing approximately 315 kb (Figs. 3B, C). There are no recombination events between the mutation and microsatellite D, indicating very tight linkage to the mutation. Only 3 genes are located within this region according to version 5 of the zebrafish genome (Sanger Center Zv5, December 2005): TTN_1, *FKBP7*, and the Ensembl-predicted gene *ENSDARG00000031678*, which appears to be loosely orthologous to mammalian collagen type V (Fig. 3). The latter two have been sequenced and show no mutations in exons, intron/exon boundaries, or known 5′ and 3′ untranslated regions, further suggesting that the causative mutation lies within the TTN_1 gene.

To test titin proteins for alteration in 6.5 dpf *ruz* mutants, we performed indirect immunofluorescence using anti-titin clone T11 antibodies. In wild-type fish, titin expression appears as a regular banded pattern showing alignment between the sarcomeres of adjacent myofibrils (Fig. 4A). *ruz* mutant, however, have severely decreased titin immunofluorescence when imaged for the same exposure time (Fig. 4B), demonstrating either a decrease of overall titin expression or of a specific isoform(s) recognized by the T11 antibody. Analysis of other sarcomeric proteins, including actin and nebulin, shows decreased muscle organization and fewer apparent sarcomeres but do not demonstrate the decrease in expression levels apparent with titin antibodies (Figs. 2E–H). Severe reduction of titin protein levels in combination with the genetic linkage data most strongly implicates titin as the gene mutated to cause the *ruz* phenotype.

Striated skeletal muscles of other animals are known to express multiple isoforms of titin. To analyze zebrafish titin isoforms and determine if specific isoforms are affected, a denaturing 1% agarose/glycerol gel was used to electrophoretically separate large proteins of striated muscle according to

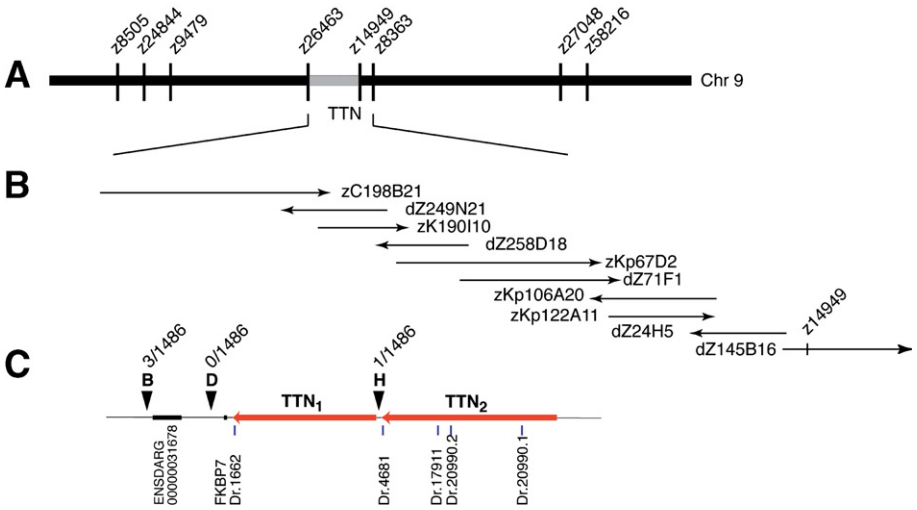

Fig. 3. Localization of the *ruz* mutation. (A) The *ruz* mutation was mapped using linkage analysis to Chr 9 between microsatellite markers z26463 and z14949. Previous studies located *TTN* between z26463 and z8363 (Xu et al., 2002). (B) Exons of human cardiac titin were used to identify zebrafish BAC sequences *in silico* and create a contig overlapping the titin region. Further searches of the Sanger Center BAC sequences allowed extension of the contig to z14949. (C) The zebrafish titin gene locus is duplicated with loci arranged head to tail. The alignment of TTN_1 and TTN_2 with the BAC contig is shown. Higher resolution genetic mapping using 1486 meioses places the *ruz* mutation between microsatellites B and H, containing the entire TTN_1 locus. The predicted genes *ENSDARG00000031678* and *FKBP7* are also in this interval but contain no mutations. Numbers of recombinations per meioses are indicated above each microsatellite. Affymetrix zebrafish titin probes are indicated below the *TTN* loci.

Warren et al. (2003a,b). India ink staining can be used to detect titin isoforms since all other known proteins are significantly smaller. (The next largest proteins, nebulin and obscurin, have estimated sizes of approximately 800 kDa, roughly 0.2–0.25× the size of titin.) Western blot analysis was also attempted but none of the tested titin antibodies cross-reacted with zebrafish titin on immunoblot.

Surprisingly, India ink staining of wild-type fish lysates showed drastic alteration of titin isoforms during development. Significant expression of full-length titin was not seen in 1 dpf fish (data not shown). By 2 dpf, when fish are able to move but are typically still within the chorion, low levels of expression of at least 5 titin isoforms are detected (Fig. 4C). At least two of these isoform sizes are not represented at any other embryonic stage of zebrafish development (Fig. 4C and data not shown). At 3–3.5 dpf when fish typically emerge from the chorion, wild-type skeletal muscle expresses four distinct sizes of titin isoforms. These four isoforms group as two doublets, the largest of which appear to be the slowest migrating zebrafish skeletal muscle titin isoforms expressed during the first week of development. A second change in titin isoform size and number begins between 4 and 5 dpf (data not shown). By 6.5 dpf, only two lower molecular weight titin isoforms are expressed in wild-type zebrafish muscle (Fig. 4C). In particular, strongest expression is seen of the larger isoform at this stage. While it is possible that the smaller detected isoform is a T2 degradation product, it is unlikely due to its size compared with human psoas muscle isoforms and the lack of similar isoforms at 3.5 dpf. These studies demonstrate a previously unrecognized rapid alteration of titin isoforms during skeletal muscle development.

Similar analysis of *ruz* mutant protein lysates suggests that titin isoforms are affected by the *ruz* mutation. At 3–3.5 dpf when the *ruz*phenotype is first visible, all four isoforms are present though mutants express slightly decreased amounts of the largest two titin isoforms. At 6.5 dpf when *ruz* mutants are unable to maintain coordinated swimming movements, a strong decrease is apparent in the larger 6.5-day isoform (Fig. 4C, arrows), suggesting isoform-specific disruption.

To further support a causative TTN_1 mutation for the *ruz* phenotype, two non-overlapping antisense morpholinos were used in separate experiments to specifically knock-down expression from the TTN_1 locus in wild-type zebrafish embryos. TTN_1 morphants hatch from the chorion significantly slower than uninjected siblings (<30% at 3.5 dpf compared with 90% of wild-type siblings in three independent experiments using the TTN1a morpholino) and are overall smaller than their uninjected or invert morpholino-injected siblings. While all morphants were capable of muscle contraction, greater than 90% of 3.5 dpf TTN_1 morphants demonstrated decreased muscle birefringence and showed impaired directional escape mobility, phenocopying the primary phenotypes of the *ruz* mutant (Fig. 5A and data not shown). Decreased birefringence was not seen in either the uninjected siblings or inverted control morpholino-injected siblings (Fig. 5A and data not shown). A higher number of TTN_1 morphants also presented with cardiac edemas than did the controls, suggesting that the TTN_1 locus may also be required during normal cardiac development. These phenotypes are similar to those recently reported for morpholino downregulation of the TTN_1 N2A exon splice site, an exon that is expressed in both skeletal and cardiac muscle titin isoforms (Seeley et al., 2006).

India ink staining of protein lysates from 3.5 dpf TTN_1 morphants demonstrates a specific downregulation of the same titin isoforms affected by the *ruz* mutation (Fig. 5B). Furthermore, the absence of the upper doublet in TTN_1 morphants

Table 1
ruz transcriptome alteration

Affymetrix ID	Fold change	*q*	Gene homolog
Dr.13265.1.A1_at	7.69	0.00	Hsp70
Dr.152.1.A1_at	5.20	0.00	Cmya1
Dr.19613.1.S1_at	5.17	0.01	Similar to KIAA002
Dr.342.1.S1_at	4.33	0.05	Wnt10a
Dr.2619.1.S2_at	3.28	0.02	Rbmx
Dr.12378.1.S1_at	2.98	0.00	Hspb1
Dr.19937.1.S2_at	2.95	0.02	Npm1
Dr.21800.1.A1_at	2.63	0.00	MbpC (Fast skeletal muscle isoform)
Dr.20198.2.S1_x_at	2.49	0.02	Similar to hsp70
Dr.17111.1.A1_at	2.40	0.00	Similar to ubiquitin protease 5M37
Dr.345.1.S1_at	2.39	0.00	Unc-45 related
Dr.15964.1.A1_at	2.16	0.00	Similar to Doc1
Dr.14522.1.S1_at	2.16	0.00	Parva4a
Dr.10870.1.S1_at	2.13	0.03	Mta3
Dr.20990.2.S1_at	1.95	0.00	Titin
Dr.34.1.S1_at	1.89	0.00	Desmin
Dr.542.1.S1_at	1.84	0.03	Mdm2
Dr.610.1.S1_at	1.83	0.00	Hsp90a
Dr.1289.1.S1_at	1.83	0.00	Similar to complement 32
Dr.9702.1.S1_at	1.82	0.00	C12ORF51
Dr.610.2.S1_a_at	1.77	0.00	Hsp90a
Dr.4495.2.S1_at	1.75	0.01	Dystrophin
Dr.3713.1.A1_at	1.75	0.01	Filamin C
Dr.16392.1.A1_at	1.74	0.05	Complement component 6
Dr.12491.1.A1_at	1.68	0.05	Complement component 4
Dr.10326.1.S1_at	1.67	0.03	JunB
Dr.24233.1.S1_at	1.64	0.02	Fibronectin 1b
Dr.24562.1.S1_a_at	1.61	0.02	Major vault protein
Dr.523.1.A1_at	1.60	0.00	eEF2k
Dr.19602.1.S1_at	−3.64	0.03	Desmin
Dr.24899.1.A1_at	−2.37	0.00	Keratin alpha-2
Dr.1361.1.S1_at	−2.22	0.00	Keratin type I, K15
Dr.20277.1.A1_at	−2.11	0.00	Acta2
Dr.25556.1.S1_at	−2.08	0.00	Keratin type I
Dr.24487.1.A1_at	−2.01	0.00	Keratin gamma-3
Dr.17976.1.S1_at	−1.95	0.01	MCG4172
Dr.20602.1.S1_at	−1.91	0.00	Transgelin, smooth muscle
AFFX-Dr-acta1-5_at	−1.84	0.00	Skeletal muscle actin
Dr.20337.1.S1_at	−1.78	0.05	Annexin A2b
Dr.1662.1.S1_at	−1.71	0.00	Titin
Dr.3448.1.S1_at	−1.63	0.02	Kruppel-like factor 2a
Dr.20990.2	1.95	0.00	Titin
Dr.4681.1	1.54	0.01	Titin N2-B
Dr.1662.1	−1.72	0.00	Titin N2-B
Dr.17911.1	NA		Titin N2-A
Dr.20990.1	NA		Titin N2-A

Three independent RNA samples were extracted from pooled tail tissue of 3.5 dpf *ruz* mutants or wild-type siblings, labeled, and hybridized to Affymetrix zebrafish chips. Data were analyzed according to Choe et al. (2005) and filtered to include probes with fold changes ≥1.6 with significance values of $q \leq 0.05$. Probes with available ortholog information are shown. All five probes corresponding to titin isoforms are listed separately.

suggests that both of the larger isoforms visible at 3.5 dpf are encoded by the TTN_1 locus whereas the two smaller isoforms are likely encoded by TTN_2. Additional histological analysis of TTN_1 morphant muscle demonstrates decreased alignment of muscle fibers and atypical nuclei, comparable to that seen in *ruz* mutants (Figs. 1 and 5C, D). The increased severity of the TTN_1 morphant phenotype, including cardiac abnormalities not seen in *ruz* mutants, may be due to differences in the timing or to some extent the degree of TTN_1 expression loss (compare Fig. 4C with Fig. 5B).

Ultrastructural effects of the ruz mutation

Titin is a major structural protein of the muscle sarcomere and is required for proper sarcomerogenesis and maintenance of M line localization. To examine the ultrastructural effect of *ruz* titin isoform loss, wild-type and *ruz* mutant skeletal muscles were analyzed using transmission electron microscopy. At 3.5 dpf, *ruz* mutants show the first phenotypic birefringence changes (Fig. 1), correlating with mild reduction of the largest two titin isoforms detected during development (Fig. 4C). By electron microscopy, mutant muscle contains regions of largely normal sarcomeric structure at this time (Figs. 6A, B). However, there is also evidence of sarcomeric disruption to varying degrees (Fig. 6C). By 6.5 dpf, *ruz* mutants show little to no directional swimming ability and severe reduction of the larger remaining titin isoform (Fig. 4C). At this time point, only rare patches of myofibrillar alignment could be found ultrastructurally (Figs. 6E, F). Instead, much of the fiber is composed of electron dense structures that appear to be collapsed myofibrils containing sarcomeric units but lacking any alignment (Figs. 6G, H). From 3.5 to 6.5 dpf, wild-type muscle sarcomeres are likely remodeled to contain lower molecular weight titin isoforms as seen in Fig. 4C. Mutant muscle, however, shows a progressive sarcomeric disruption which may result either from faulty sarcomeric remodeling during this period, or from specific loss of function of the affected titin isoforms.

ruz transcriptome changes

To determine transcriptional changes caused by the *ruz* mutation, we performed Affymetrix microarray analysis in triplicate, comparing *ruz* mutant skeletal muscle with wild-type siblings at the onset of the visible phenotype. Eighty-two genes were upregulated in mutant muscle by more than 1.6-fold ($q \leq 0.05$), 29 of them with identified mammalian orthologs (Table 1). Thirty-four genes were decreased more than 1.6-fold ($q \leq 0.05$), 12 of which have identified mammalian orthologs. Additional orthologs may not have been detected based on locations of given probe set sequences.

Six of the 29 upregulated gene orthologs are known to be expressed in muscle, including dystrophin, desmin, and filamin C, all of which can cause mammalian muscle diseases when mutated. The most highly upregulated gene, however, is the molecular chaperone hsp70. Four additional heat shock proteins are also significantly upregulated in *ruz* mutant skeletal muscle. The largest group of proteins decreased in *ruz* at 3.5 dpf are keratins, comprising 4 out of the 12 genes with known mammalian orthologs and perhaps denoting a secondary skin phenotype in *ruz* mutants. Additional genes include the striated muscle gene desmin (suggesting diverse effects of the mutation on different desmin isoforms) and the smooth muscle genes acta2 and transgelin.

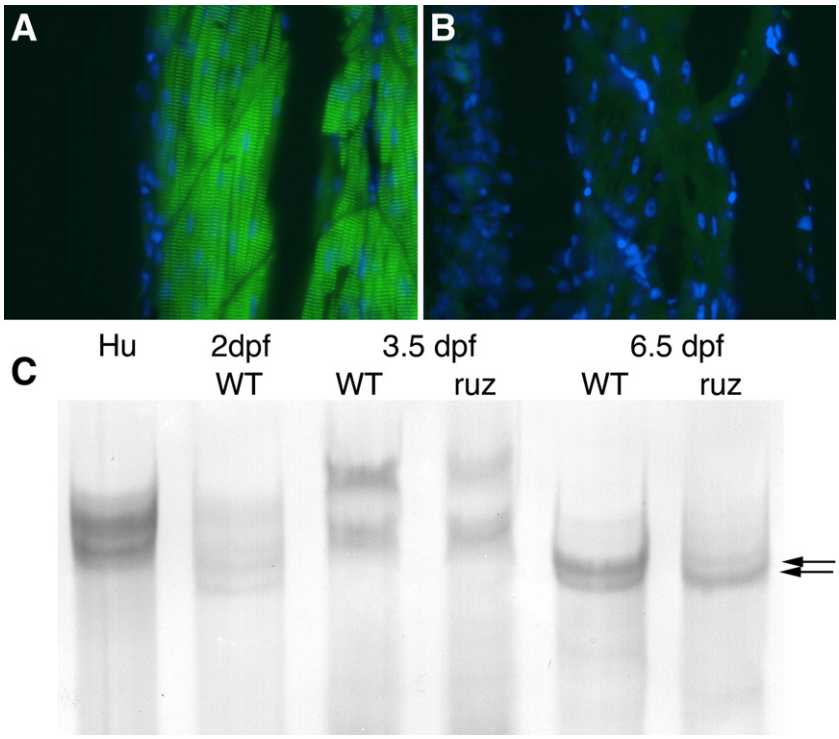

Fig. 4. *ruz* mutants exhibit decreased expression of specific titin isoforms. (A, B) Indirect immunofluorescence was performed on skeletal muscle longitudinal sections at 6 dpf. Nuclei were stained with DAPI (blue). (A) Wild-type muscle shows titin expression in a repeating sarcomeric pattern. (B) Mutant muscle shows severely decreased titin expression when imaged for the same exposure time. (C) Protein lysates of human psoas muscle (Hu), 2 dpf, 3.5 dpf, and 6.5 dpf wild-type (WT) zebrafish, and 3.5 dpf and 6.5 dpf *ruz* mutants (*ruz*) were separated by electrophoresis in adjacent wells of an SDS–agarose gel, transferred to nitrocellulose, and stained with India ink. Lysates loaded either by equal tissue weight per lysis volume or by equal total protein amount showed identical results. At 2 dpf, five faint titin isoforms are apparent. By 3.5 dpf, wild-type fish express four titin isoforms, including two isoforms with the lowest mobility seen during embryonic development. The low mobility doublet is slightly decreased in *ruz* mutants. At 6.5 dpf, wild-type zebrafish express two titin isoforms (arrows). The larger isoform is severely reduced in *ruz* mutants while the smaller variant appears increased. Identical results were seen in three independent experiments.

The zebrafish Affymetrix gene chip contains 5 probe sets against titin which may recognize different titin isoforms (Fig. 3C). Table 1 (bottom) shows transcriptional changes in these probes along with their Affymetrix-suggested isoform identities. Both Dr.4681.1 and Dr.20990.2, which show upregulation in *ruz* mutants, are located in TTN_2. In addition, two probes that show no alteration in expression are located in TTN_2, perhaps indicating multiple splice isoforms of the TTN_2 gene locus. The only reduced titin probe, Dr.1662.1, is also the only probe within the TTN_1 locus, further implicating the TTN_1 locus as a primary alteration of the *ruz* mutation. Decreases in TTN_1 transcripts containing the Dr.1662.1 probe sequence were confirmed by quantitative RT-PCR (data not shown).

ruz comparison with known titinopathies

Few specific alterations have been noted in mammalian skeletal muscle titinopathies, but the most notable is a decrease or loss of calpain-3. Using Western blot analysis, however, no decrease in calpain-3 expression was seen in *ruz* mutant fish (Fig. 7A). In fact, mild increases were detected, suggesting a new mechanism of dystrophy pathogenesis in the *ruz* mutant. Additional mammalian titinopathy effects have been identified in murine *mdm* skeletal muscle using microarray analysis, specifically the upregulation of several ankyrin-containing proteins (Witt et al., 2004). To determine if *ruz* pathology showed similar increases, expression of CARP and ankrd2 (two transcripts with the greatest increases in *mdm*) was investigated by quantitative RT-PCR. Neither gene was found to be affected (data not shown).

In the HMERF titinopathy, mutations in the titin kinase domain cause displacement of scaffolding proteins and the muscle ring-finger protein, MuRF2, from the sarcomere in skeletal muscle culture. Subsequent nuclear translocation of MuRF2 in turn decreases muscle gene transcription (Lange et al., 2005). We thus assayed changes in MuRF2 localization using indirect immunofluorescence in *ruz* skeletal muscle. In wild-type muscle, MuRF2 is primarily localized to the sarcomere though nuclear overlap is seen (Fig. 7B). In mutant skeletal muscle, MuRF2 is lost at the sarcomere but remains primarily within the cytoplasm. No apparent nuclear translocation is detected of either MuRF2 (Fig. 7C) or of MuRF1 (data not shown), suggesting that the *ruz* mutation results in structural or signaling pathway alterations unperturbed in known titinopathies.

Discussion

Titin protein is thought to provide a scaffold for development of the sarcomere in striated muscle. In mature muscle, titin also

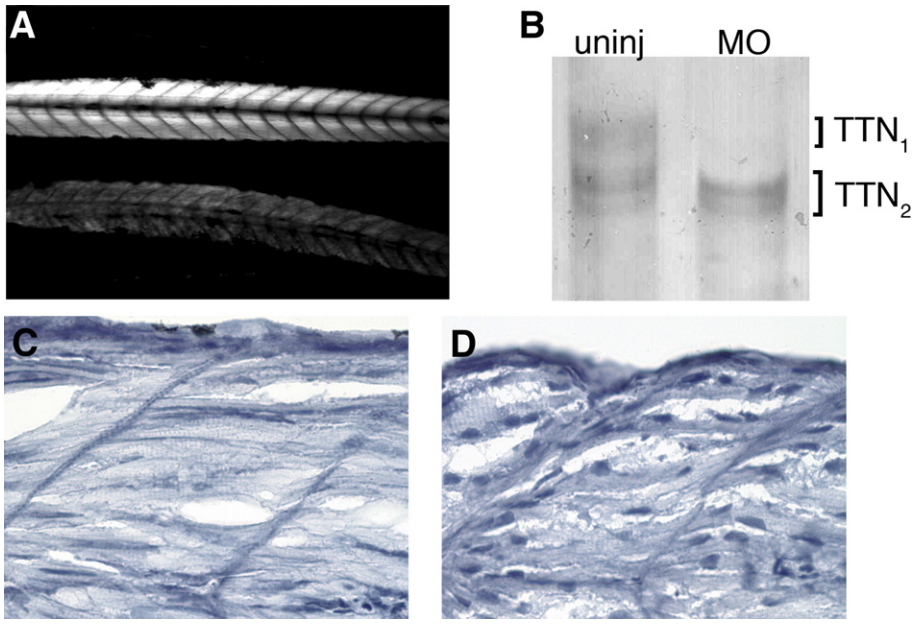

Fig. 5. Morpholinos against TTN_1 phenocopy the *ruz* mutation. (A) 3.5 dpf wild-type fish injected with the TTN1b morpholino against the translational start site of TTN_1 (bottom) show decreased birefringence, mobility, and size and are slow to hatch compared with uninjected wild-type siblings (top). Similar results were seen upon injection with the non-overlapping TTN1a morpholino compared with inverted control-injected siblings (data not shown). (B) India ink staining of electrophoretically separated protein lysates of 3.5 dpf TTN1a morphants (MO) and uninjected siblings (uninj) shows loss of the two largest titin isoforms in TTN_1 morphants. Smaller titin isoforms are thus likely coded by the adjacent TTN_2 gene. (C, D) Longitudinal sections of zebrafish skeletal muscle at 3.5 dpf were stained with hematoxylin. (C) Wild-type muscle shows myofiber alignment between myosepta and peripherally localized nuclei. (D) TTN1a morphants have decreased myofiber alignment and abnormally shaped nuclei similar to *ruz* mutants.

provides passive forces, maintains correct localization of M lines, and binds many potential signaling and structural molecules. Mutations in at least three locations within the gene have been correlated with human and murine muscular dystrophies. Here, we show that the *ruz* muscle phenotype in zebrafish is also likely caused by a mutation in the titin gene. Genetic mapping of the causative mutation determined linkage to an interval of Chr 9 that is syntenic to the titin-containing region of human chromosome 2 (Xu et al., 2002). In zebrafish, the titin gene locus appears to be duplicated with loci located immediately adjacent to one another. A recent report by Seeley et al. (2006) confirms this organization of the titin locus. The genetically linked interval for the *ruz* mutant contains one titin locus (TTN_1) and two additional genes. Both additional genes have been sequenced and excluded as candidates, implicating titin as the mutation-containing gene in *ruz* fish. Further analysis of titin at the RNA level shows reduction specifically of TTN_1-associated transcripts, strongly supporting a TTN_1-specific mutation that decreases at least one TTN_1 isoform. Immunofluorescence confirms that titin is extremely reduced in abundance in *ruz* mutant muscle while expression of other sarcomeric proteins is maintained though disorganized. Finally, two non-overlapping morpholinos designed against the TTN_1 locus phenocopy the *ruz* mutation and result in loss of the same titin isoforms decreased in the *ruz* mutant. Thus, genetic linkage, antisense knock-down, RNA studies, and protein analysis all suggest that the *ruz* mutation is located in TTN_1.

Additional protein analysis of electrophoretically separated lysates demonstrates mild decreases in the largest titin isoforms at 3.5 dpf and severe reduction of a distinct isoform at 6.5 dpf in *ruz* mutants. Consistent with these findings, ultrastructural analysis shows a progressive decline in sarcomeric alignment. Due to the high degree of repeated elements in titin, the lack of complete zebrafish titin sequences, and the large number of exons, we have not yet identified the causative base pair alteration. However, sequencing of regions corresponding to TTN_1 M line exons in zebrafish ESTs – including the regions mutated in human TMD, LGMD 2J, and HMERF – detected no mutations (data not shown). In addition, the large size of the gene precludes traditional mRNA rescue.

The *ruz* mutation represents a novel dystrophy phenotype with transcript and protein alterations distinct from known vertebrate titinopathies. The only previously published zebrafish titinopathy, pik^{m171}, results from a nonsense mutation in a cardiac-specific titin exon, preventing sarcomerogenesis entirely (Xu et al., 2002). pik^{m171} mutants confirm previous mammalian in vitro experiments suggesting that titin is required for sarcomere development. However, the lack of any similar gross cardiac defects in *ruz* mutants and the appearance of striated muscle sarcomeres suggests a distinct, skeletal muscle-specific phenotype in *ruz*. While it is not certain that mutant muscle development is entirely normal prior to 3 dpf, ultrastructural analysis demonstrates that the majority of muscle contains reasonably ordered sarcomeres and thus suggests that the primary effects of the mutation appear far later than pik^{m171}. Mutations in the kinase domain of human titin have been shown to result in human HMERF phenotypes by displacing scaffolding proteins. The resulting nuclear translocation of MuRF2 has been shown to effect downregulation of some muscle gene transcription and may play a role in myopathy pathogenesis

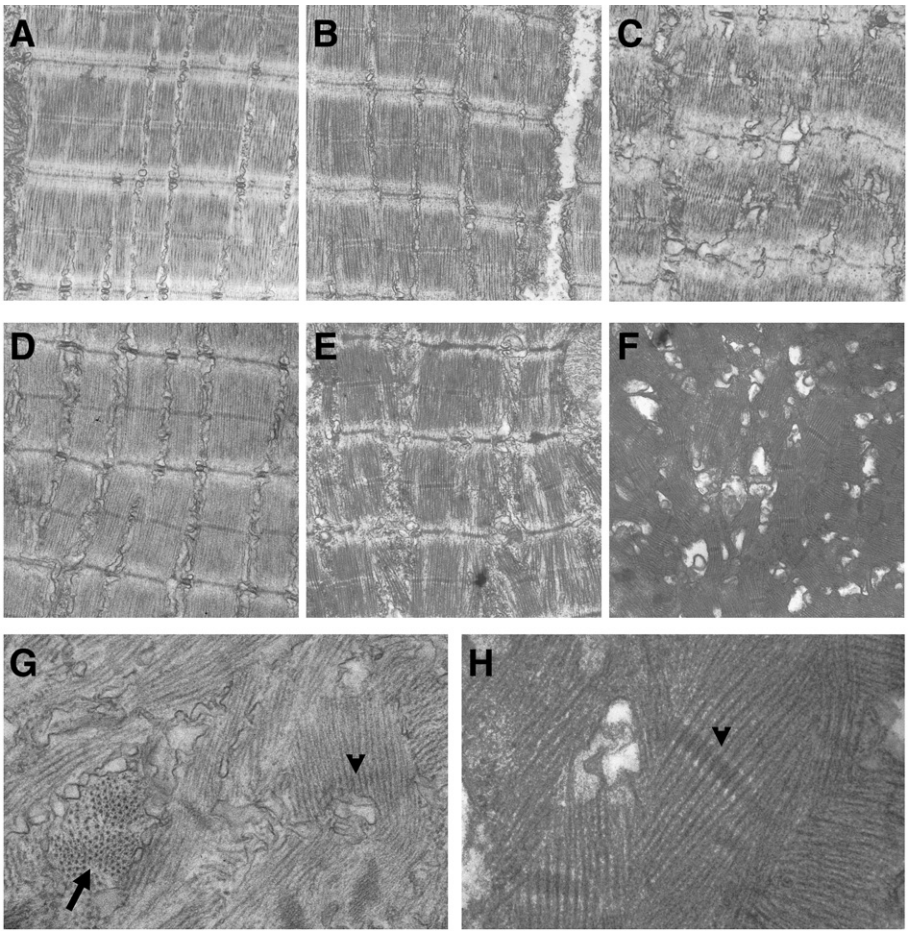

Fig. 6. *ruz* mutants produce normal sarcomeres but show progressive sarcomeric misalignment. (A–H) Longitudinal sections of skeletal muscle from 3.5 dpf (A–C) or 6.5 dpf (D–H) fish were analyzed by transmission electron microscopy. (A) Wild-type fish at 3.5 dpf show normal sarcomeric organization and alignment. (B, C) *ruz* mutants contain some normal sarcomeres at 3.5 dpf (B) but are also beginning to show sarcomeric disruption (C). At 6.5 dpf, wild-type fish still display normal sarcomeres (D) while *ruz* mutants contain only rare regions of ordered myofibrils (E). Instead, myofibers contain collapsed sarcomeres with no apparent organization or alignment (F–H). Arrow indicates fibrils perpendicular to the plane of the section. Arrowheads indicate selected Z-disc structures.

(Lange et al., 2005). We analyzed *ruz* mutant muscle for nuclear translocation of MuRF transcription factors. Displacement of MuRF2 (Figs. 3, 4, 5, 6C) (and MuRF1, data not shown) from the sarcomere was seen in *ruz* mutants, perhaps indicating a role for MuRFs in the *ruz* phenotype. However, an increase in MuRF nuclear localization was not detected nor was a significant number of muscle-specific genes reduced (Supplementary Table 1), suggesting that *ruz* pathogenesis differs from that of HMERF striated muscle.

Of the other skeletal muscle titinopathies, both the human LGMD2J and murine *mdm* phenotypes are early onset, recessive diseases with a severity of phenotype and shortened lifespan most similar to *ruz*. Both of these mutations affect calpain-3, resulting in loss of calpain-3 binding and a decrease or complete loss of calpain-3 expression (Hackman et al., 2002; Haravuori et al., 2001). In *ruz* fish, calpain-3 instead appears to be mildly upregulated, perhaps representing a previously unknown ability of titin to negatively regulate calpain-3 expression. Alternatively, the increase in calpain-3 may be dependent on the modest increases seen in the TTN_2 locus as shown by both microarray and protein analyses. Additional defects identified in the *mdm* mouse model, namely increases in CARP and ankrd2 (Witt et al., 2004), were absent in *ruz* muscle as seen by quantitative RT-PCR (data not shown). Lack of increase in CARP and ankrd2 further suggests that the putative *ruz* titinopathy does not occur through previously known mechanisms.

Instead, alteration of the heat shock proteins is likely to be a specific hallmark of the *ruz* dystrophy. Previous research has shown that heat shock proteins display tissue-specific expression during zebrafish embryonic development, with hsp90a localized to skeletal muscle progenitors (Krone et al., 2003). It is possible that the increases seen in hsp90a transcripts in *ruz* mutants may be part of the dystrophic cycle of degeneration and regeneration with specificity to the *ruz* mutation. Further analysis of hsps in human patients with muscular dystrophies of unknown origin may identify similar titinopathies in mammals.

Previous studies have documented numerous isoforms of the titin gene, depending primarily on the organism and muscle group being studied. In cardiac muscle, Lahmers et al. (2004) have shown developmental regulation of titin isoform expression. A similar study in chicken skeletal muscle has shown a change of titin isoforms between pre- and post-natal muscle (Hattori et al., 1995). To our knowledge, the current study is the

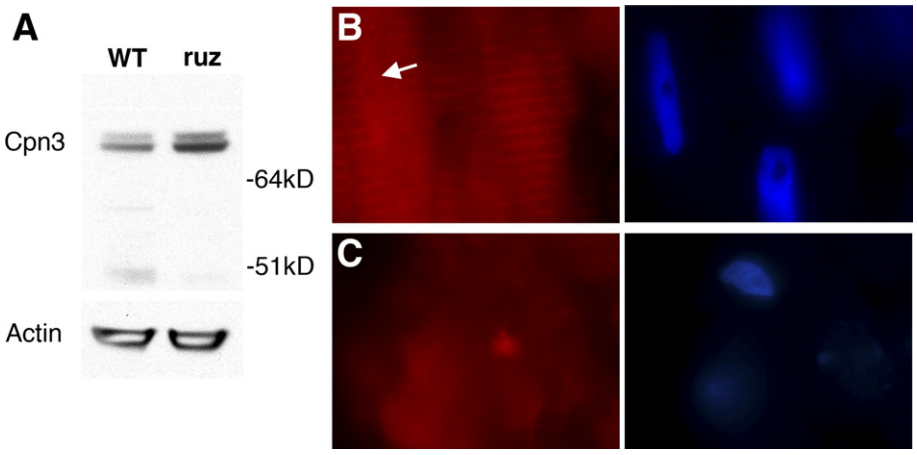

Fig. 7. The *ruz* dystrophy shows increased calpain-3 and loss of sarcomeric MuRF2 expression. (A) Western blot analysis of 6.5 dpf wild-type and *ruz* mutants shows a mild increase in calpain-3. Actin expression is used as a loading control. (B, C) Indirect immunofluorescence using MuRF2 antibodies (red) was performed on longitudinally sectioned skeletal muscle of 6.5 dpf fish. Nuclei were stained with DAPI (blue). (B) In wild-type fish, MuRF2 is localized to both the sarcomere (striations) and nucleus (arrow). (C) MuRF2 is lost at the sarcomere in *ruz* mutants but no significant increase in nuclear localization is detected.

first to show that titin isoforms in vertebrate skeletal muscle are modified throughout embryonic development. A total of 9–11 distinct size variants of titin are present in zebrafish skeletal muscle between 2 and 6.5 dpf (Figs. 3 and 4C). While it is unclear if all size variants represent developmentally regulated transcriptional or splicing changes (as opposed to post-translational modification), the appearance of two significantly larger isoforms at 3–3.5 dpf supports transcript alteration for at least some of the size variants. Our immunofluorescence data and others have also shown that titin protein is organized within the sarcomere throughout this time (Costa et al., 2002). Together, this suggests a previously unrecognized rapid ability of the sarcomere to remodel between 2 and 3.5 dpf to replace earlier titin molecules with the developmentally regulated large titin isoforms. It is also interesting to note that alternative splicing of titin exons during development may explain previously seen changes in titin epitope accessibility in studies of developing muscle (Rudy et al., 2001).

In addition to isoform switching during normal zebrafish muscle development, Figs. 3 and 4C show changes in titin mobility due to the *ruz* mutation. Correlating with the progressive severity of the visible and ultrastructural phenotypes, *ruz* mutants demonstrate a progressive reduction of the largest titin isoforms, with mild decreases seen at 3.5 dpf and near loss seen at 6.5 dpf. These alterations may indicate loss of titin modifications or perhaps a specific titin degradation event. However, because the smaller isoforms are also present in freshly prepared wild-type embryo lysates, it is more likely that the mobility differences represent isoform expression changes due to the *ruz* mutation. Titin isoform changes with disease status have previously been detected in cardiac tissues of patients and animal models with DCM (Nagueh et al., 2004; Wu et al., 2002). Changes in titin mobility have also been detected in Fukuyama muscular dystrophy and DMD, though the electrophoretic techniques used do not allow distinction of individual isoforms. To our knowledge, this is the first example of a putative titinopathy that specifically decreases one titin isoform. This may be due to separation of the isoform origins into two distinct loci, only one of which contains the mutation.

At 3.5 dpf, titin expression was also analyzed at the mRNA level using the zebrafish Affymetrix chip containing five distinct titin probes. Results indicate that a titin isoform(s) corresponding to the Dr.1662 probe sequence within TTN_1 is decreased in mutants (Supplementary Table 1) and have been confirmed by quantitative RT-PCR (data not shown). Compensatory upregulation is seen in two additional titin probes from the TTN_2 locus, while the remaining two TTN_2 probes show no significant change. Further RT-PCR analysis of gene products from the zebrafish titin locus will be required to identify the full-length identity of isoforms corresponding to each titin locus. However, the NCBI databases currently show two distinct partial transcripts (BC095863 and XM_677962) containing the Dr.1662 probe, which may correspond to the higher molecular weight titin products detected (and reduced) at 3.5 dpf from the TTN_1 locus. Likewise, it will be interesting to determine the mechanism of regulation and feedback involved in isoform determination for the duplicated zebrafish titin locus. Even for the single mammalian titin locus, regulation of differential isoform splicing has not been identified.

Decades of research using the vertebrate zebrafish *D. rerio* have demonstrated many similarities with mammalian muscle organization and development. We have taken advantage of this model to further understand the role of titin in skeletal muscle and muscle disease. This study demonstrates a rapid change in titin isoforms during embryonic development of the skeletal muscle, likely involving remodeling of the sarcomere to effect the exchange of titin proteins. Study of the zebrafish *ruz* muscular dystrophy mutant also suggests that these isoforms may have separable functions, since initial sarcomerogenesis appears to be largely unaffected but maintenance of myofibrillar alignment is lost upon reduction of certain titin isoforms. Comparison with mammalian titinopathies shows that *ruz* represents a novel putative titinopathy, with mild increases in heat shock protein transcripts and calpain-3. Further sequencing is required to determine the organization of the zebrafish titin

locus, exon content of titin isoforms, and the exact location of the *ruz* mutation.

Acknowledgments

LSS, JRG, EDV, and LMK are supported by a grant from the Bernard F. and Alva B. Gimbel Foundation. JRG was also supported by a grant from the Muscular Dystrophy Association. GJW, YZ, and LIZ are supported by a genome grant from the NIDDK. LIZ and LMK are investigators with Howard Hughes Medical Institute. Sequencing was performed at the Molecular Genetics Core Facility at Children's Hospital under an MRDDRC grant (NIH-P30-HD18655).

Appendix A. Supplementary data

Supplementary data associated with this article can be found, in the online version, at doi:10.1016/j.ydbio.2007.06.015.

References

Bahary, N., Davidson, A., Ransom, D., Shepard, J., Stern, H., Trede, N., Zhou, Y., Barut, B., Zon, L.I., 2004. The Zon laboratory guide to positional cloning in zebrafish. Methods Cell Biol. 77, 305–329.

Bang, M.L., Centner, T., Fornoff, F., Geach, A.J., Gotthardt, M., McNabb, M., Witt, C.C., Labeit, D., Gregorio, C.C., Granzier, H., et al., 2001. The complete gene sequence of titin, expression of an unusual approximately 700-kDa titin isoform, and its interaction with obscurin identify a novel Z-line to I-band linking system. Circ. Res. 89, 1065–1072.

Bassett, D.I., Currie, P.D., 2003. The zebrafish as a model for muscular dystrophy and congenital myopathy. Hum. Mol. Genet. 12, R265–R270 (Spec No 2).

Bassett, D.I., Bryson-Richardson, R.J., Daggett, D.F., Gautier, P., Keenan, D.G., Currie, P.D., 2003. Dystrophin is required for the formation of stable muscle attachments in the zebrafish embryo. Development 130, 58510–58560.

Cazorla, O., Freiburg, A., Helmes, M., Centner, T., McNabb, M., Wu, Y., Trombitas, K., Labeit, S., Granzier, H., 2000. Differential expression of cardiac titin isoforms and modulation of cellular stiffness. Circ. Res. 86, 59–67.

Choe, S.E., Boutros, M., Michelson, A.M., Church, G.M., Halfon, M.S., 2005. Preferred analysis methods for Affymetrix GeneChips revealed by a wholly defined control dataset. Genome Biol. 6, R16.

Costa, M.L., Escaleira, R.C., Rodrigues, V.B., Manasfi, M., Mermelstein, C.S., 2002. Some distinctive features of zebrafish myogenesis based on unexpected distributions of the muscle cytoskeletal proteins actin, myosin, desmin, alpha-actinin, troponin and titin. Mech. Dev. 116, 95–104.

Dodd, A., Chambers, S.P., Love, D.R., 2004. Short interfering RNA-mediated gene targeting in the zebrafish. FEBS Lett. 561, 89–93.

Freiburg, A., Trombitas, K., Hell, W., Cazorla, O., Fougerousse, F., Centner, T., Kolmerer, B., Witt, C., Beckmann, J.S., Gregorio, C.C., et al., 2000. Series of exon-skipping events in the elastic spring region of titin as the structural basis for myofibrillar elastic diversity. Circ. Res. 86, 1114–1121.

Furst, D.O., Osborn, M., Nave, R., Weber, K., 1988. The organization of titin filaments in the half-sarcomere revealed by monoclonal antibodies in immunoelectron microscopy: a map of ten nonrepetitive epitopes starting at the Z line extends close to the M line. J. Cell Biol. 106, 1563–1572.

Gerull, B., Atherton, J., Geupel, A., Sasse-Klaassen, S., Heuser, A., Frenneaux, M., McNabb, M., Granzier, H., Labeit, S., Thierfelder, L., 2006. Identification of a novel frameshift mutation in the giant muscle filament titin in a large Australian family with dilated cardiomyopathy. J. Mol. Med. 84, 478–483.

Granato, M., van Eeden, F.J., Schach, U., Trowe, T., Brand, M., Furutani-Seiki, M., Haffter, P., Hammerschmidt, M., Heisenberg, C.P., Jiang, Y.J., et al., 1996. Genes controlling and mediating locomotion behavior of the zebrafish embryo and larva. Development 123, 399–413.

Gregorio, C.C., Trombitas, K., Centner, T., Kolmerer, B., Stier, G., Kunke, K., Suzuki, K., Obermayr, F., Herrmann, B., Granzier, H., et al., 1998. The NH_2 terminus of titin spans the Z-disc: its interaction with a novel 19-kD ligand (T-cap) is required for sarcomeric integrity. J. Cell Biol. 143, 1013–1027.

Guyon, J.R., Mosley, A.N., Zhou, Y., O'Brien, K.F., Sheng, X., Chiang, K., Davidson, A.J., Volinski, J.M., Zon, L.I., Kunkel, L.M., 2003. The dystrophin associated protein complex in zebrafish. Hum. Mol. Genet. 12, 601–615.

Guyon, J.R., Mosley, A.N., Jun, S.J., Montanaro, F., Steffen, L.S., Zhou, Y., Nigro, V., Zon, L.I., Kunkel, L.M., 2005. Delta-sarcoglycan is required for early zebrafish muscle organization. Exp. Cell Res. 304, 105–115.

Hackman, P., Vihola, A., Haravuori, H., Marchand, S., Sarparanta, J., De Seze, J., Labeit, S., Witt, C., Peltonen, L., Richard, I., et al., 2002. Tibial muscular dystrophy is a titinopathy caused by mutations in TTN, the gene encoding the giant skeletal-muscle protein titin. Am. J. Hum. Genet. 71, 492–500.

Haravuori, H., Vihola, A., Straub, V., Auranen, M., Richard, I., Marchand, S., Voit, T., Labeit, S., Somer, H., Peltonen, L., 2001. Secondary calpain3 deficiency in 2q-linked muscular dystrophy: titin is the candidate gene. Neurology 56, 869–877.

Hattori, A., Ishii, T., Tatsumi, R., Takahashi, M., 1995. Changes in the molecular types of connectin and nebulin during development of chicken skeletal muscle. BBA 1244, 179–184.

Huebsch, K.A., Kudryashova, E., Wooley, C.M., Sher, R.B., Seburn, K.L., Spencer, M.J., Cox, G.A., 2005. Mdm muscular dystrophy: interactions with calpain 3 and a novel functional role for titin's N2A domain. Hum. Mol. Genet. 14, 2801–2811.

Itoh-Satoh, M., Hayashi, T., Nishi, H., Koga, Y., Arimura, T., Koyanagi, T., Takahashi, M., Hohda, S., Ueda, K., Nouchi, T., et al., 2002. Titin mutations as the molecular basis for dilated cardiomyopathy. Biochem. Biophys. Res. Commun. 291, 385–393.

Kimmel, C.B., Ballard, W.W., Kimmel, S.R., Ullmann, B., Schilling, T.F., 1995. Stages of embryonic development of the zebrafish. Dev. Dyn. 203, 253–310.

Knoll, R., Hoshijima, M., Hoffman, H.M., Person, V., Lorenzen-Schmidt, I., Bang, M.L., Hayashi, T., Shiga, N., Yasukawa, H., Schaper, W., et al., 2002. The cardiac mechanical stretch sensor machinery involves a Z disc complex that is defective in a subset of human dilated cardiomyopathy. Cell 111, 943–955.

Krone, P.H., Evans, T.G., Blechinger, S.R., 2003. Heat shock gene expression and function during zebrafish embryogenesis. Semin. Cell Dev. Biol. 14, 267–274.

Lahmers, S., Wu, Y., Call, D.R., Labeit, S., Granzier, H., 2004. Developmental control of titin isoform expression and passive stiffness in fetal and neonatal myocardium. Circ. Res. 94, 505–513.

Lange, S., Xiang, F., Yakovenko, A., Vihola, A., Hackman, P., Rostkova, E., Kristensen, J., Brandmeier, B., Franzen, G., Hedberg, B., et al., 2005. The kinase domain of titin controls muscle gene expression and protein turnover. Science 308, 1599–1603.

Maruyama, K., 1976. Connectin, an elastic protein from myofibrils. J. Biochem. (Tokyo) 80, 405–407.

Miller, G., Musa, H., Gautel, M., Peckham, M., 2003. A targeted deletion of the C-terminal end of titin, including the titin kinase domain, impairs myofibrillogenesis. J. Cell Sci. 116, 4811–4819.

Nagueh, S.F., Shah, G., Wu, Y., Torre-Amione, G., King, N.M., Lahmers, S., Witt, C.C., Becker, K., Labeit, S., Granzier, H.L., 2004. Altered titin expression, myocardial stiffness, and left ventricular function in patients with dilated cardiomyopathy. Circulation 110, 155–162.

Obermann, W.M., Gautel, M., Steiner, F., van der Ven, P.F., Weber, K., Furst, D.O., 1996. The structure of the sarcomeric M band: localization of defined domains of myomesin, M-protein, and the 250-kD carboxy-terminal region of titin by immunoelectron microscopy. J. Cell Biol. 134, 1441–1453.

Prado, L.G., Makarenko, I., Andresen, C., Kruger, M., Opitz, C.A., Linke, W.A., 2005. Isoform diversity of giant proteins in relation to passive and active contractile properties of rabbit skeletal muscles. J. Gen. Physiol. 126, 461–480.

Rudy, D.E., Yatskievych, T.A., Antin, P.B., Gregorio, C.C., 2001. Assembly of

thick, thin, and titin filaments in chick precardiac explants. Dev. Dyn. 221, 61–71.

Sato, T., Mishina, M., 2003. Representational difference analysis, high-resolution physical mapping, and transcript identification of the zebrafish genomic region for a motor behavior. Genomics 82, 218–229.

Seeley, M., Huang, W., Chen, Z., Wolff, W.O., Lin, X., Xu, X., 2006. Depletion of zebrafish titin reduces cardiac contractility by disrupting the assembly of Z-discs and A-bands. Circ. Res.

Shepard, J.L., Amatruda, J.F., Stern, H.M., Subramanian, A., Finkelstein, D., Ziai, J., Finley, K.R., Pfaff, K.L., Hersey, C., Zhou, Y., et al., 2005. A zebrafish bmyb mutation causes genome instability and increased cancer susceptibility. Proc. Natl. Acad. Sci. U. S. A. 102, 13194–13199.

Tskhovrebova, L., Trinick, J., 2004. Properties of titin immunoglobulin and fibronectin-3 domains. J. Biol. Chem. 279, 46351–46354.

van der Ven, P.F., Bartsch, J.W., Gautel, M., Jockusch, H., Furst, D.O., 2000. A functional knock-out of titin results in defective myofibril assembly. J. Cell Sci. 113 (Pt. 8), 1405–1414.

Warren, C.M., Jordan, M.C., Roos, K.P., Krzesinski, P.R., Greaser, M.L., 2003a. Titin isoform expression in normal and hypertensive myocardium. Cardiovasc. Res. 59, 86–94.

Warren, C.M., Krzesinski, P.R., Greaser, M.L., 2003b. Vertical agarose gel electrophoresis and electroblotting of high-molecular-weight proteins. Electrophoresis 24, 1695–1702.

Warren, C.M., Krzesinski, P.R., Campbell, K.S., Moss, R.L., Greaser, M.L., 2004. Titin isoform changes in rat myocardium during development. Mech. Dev. 121, 1301–1312.

Weber, G.J., Choe, S.E., Dooley, K.A., Paffett-Lugassy, N.N., Zhou, Y., Zon, L.I., 2005. Mutant-specific gene programs in the zebrafish. Blood 106, 521–530.

Witt, C.C., Ono, Y., Puschmann, E., McNabb, M., Wu, Y., Gotthardt, M., Witt, S.H., Haak, M., Labeit, D., Gregorio, C.C., et al., 2004. Induction and myofibrillar targeting of CARP, and suppression of the Nkx2.5 pathway in the MDM mouse with impaired titin-based signaling. J. Mol. Biol. 336, 145–154.

Wu, Y., Bell, S.P., Trombitas, K., Witt, C.C., Labeit, S., LeWinter, M.M., Granzier, H., 2002. Changes in titin isoform expression in pacing-induced cardiac failure give rise to increased passive muscle stiffness. Circulation 106, 1384–1389.

Xu, X., Meiler, S.E., Zhong, T.P., Mohideen, M., Crossley, D.A., Burggren, W.W., Fishman, M.C., 2002. Cardiomyopathy in zebrafish due to mutation in an alternatively spliced exon of titin. Nat. Genet. 30, 205–209.